

# Differentiating hidden sector dark matter from light WIMPs with Germanium detectors

R. Foot<sup>1</sup>

*ARC Centre of Excellence for Particle Physics at the Terascale,  
School of Physics, University of Melbourne,  
Victoria 3010 Australia*

Light WIMP dark matter and hidden sector dark matter have been proposed to explain the DAMA, CoGeNT and CRESST-II data. Both of these approaches feature spin independent elastic scattering of dark matter particles on nuclei. Light WIMP dark matter invokes a single particle species which interacts with ordinary matter via contact interactions. By contrast hidden sector dark matter is typically multi-component and is assumed to interact via the exchange of a massless mediator. Such hidden sector dark matter thereby predicts a sharply rising nuclear recoil spectrum,  $dR/dE_R \sim 1/E_R^2$  due to this dynamics, while WIMP dark matter predicts a spectrum which depends sensitively on the WIMP mass,  $m_\chi$ . We compare and contrast these two very different possible origins of the CoGeNT low energy excess. In the relevant energy range, the recoil spectra predicted by these two theories approximately agree provided  $m_\chi \simeq 8.5$  GeV - close to the value favoured from fits to the CoGeNT and CDMS low energy data. Forthcoming experiments including C-4, CDEX, and the MAJORANA demonstrator, are expected to provide reasonably precise measurements of the low energy Germanium recoil spectrum, including the annual modulation amplitude, which should differentiate between these two theoretical possibilities.

---

<sup>1</sup>E-mail address: rfoot@unimelb.edu.au

# 1 Introduction

The search for dark matter via direct detection experiments continues to yield very exciting positive results. DAMA[1, 2], CoGeNT[3, 4] and CRESST-II[5] have all reported results consistent with dark matter interactions. Of these, the DAMA annual modulation signal is (currently) the most convincing evidence for dark matter direct detection. With more than 12 annual cycles of data collected, the annual modulation amplitude deviates from zero at more than  $8\sigma$  C.L. with both the phase and period consistent with dark matter expectations[6]. These are clearly very interesting times for dark matter direct detection.

Low threshold experiments can probe specific dark matter explanations of the DAMA annual modulation signal. Initial results of the CoGeNT experiment have provided some tantalizing results. Future data from C-4[7], CDEX[8] and the MAJORANA demonstrator[9], all using a Germanium target, should be able to confirm DAMA's direct detection. Furthermore, these experiments have the potential to measure both the recoil spectrum (i.e. unmodulated part) and annual modulation signal with high precision and thereby distinguish between possible dark matter candidates.

Two quite different dark matter schemes have been proposed to explain the sharply rising low energy excess seen by CoGeNT. One possibility is that this rising event rate is due to interactions of a WIMP with contact (point-like) interaction[10]. Although such an interaction predicts a flat nuclear recoil energy spectrum at low energies:  $dR/dE_R \propto \text{constant}$  as  $E_R \rightarrow 0$ , CoGeNT's low energy excess can be due to kinematic effects. For a given nuclear recoil energy  $E_R$ , only a portion of the dark matter particles in the halo have sufficient energy to produce the recoil. As  $E_R$  decreases this portion exponentially increases, yielding a sharply rising event rate at low energies. For low enough  $E_R$ , the rate should eventually flatten out producing  $dR/dE_R \propto \text{constant}$ , assuming this dark matter model is correct. Since the recoil energy dependence of the spectrum is due to kinematic effects, CoGeNT can sensitively probe the WIMP mass in this model, which comes out to around 10 GeV[11]. While light WIMPs can also potentially explain DAMA[12] and CRESST-II data[5], it appears to be a major challenge to explain all three experiments simultaneously for a consistent set of parameters[13].

There is another explanation for the sharply rising excess seen by CoGeNT. This excess might be due to dark matter particles interacting with ordinary matter via a massless mediator[14]. Dark matter arising from a hidden sector, with  $U(1)'$  gauge interaction, coupling with the ordinary matter via  $U(1)' - U(1)_Y$  kinetic mixing is one possibility[15, 16]. If the  $U(1)'$  is unbroken then the mediator is massless, and can be recognized as the photon. In this type of dark matter theory, the cross-section has a non-trivial recoil energy dependence,  $d\sigma/dE_R \propto 1/E_R^2$ . This implies  $dR/dE_R \propto 1/E_R^2$  at low energies which, it turns out[17, 18], is compatible with CoGeNT's data. In this case the dark matter particles can be heavier ( $\gtrsim 20$  GeV) as no kinematic effect is required to explain the excess. It further turns out that in this picture, denoted henceforth as hidden sector dark matter, the DAMA, CoGeNT and CRESST-II data can be simultaneously explained[17, 18].

The purpose of this article is to compare and contrast these two quite distinct

possible origins of the CoGeNT low energy excess. In particular we focus on future Germanium experiments because, as discussed above, these have the potential to measure the low energy spectrum and annual modulation amplitude with high precision.

## 2 Light WIMPs versus hidden sector dark matter

### *Light WIMPs*

Dark matter consisting of WIMP particles  $\chi$ , interacting with ordinary matter via a contact interaction is a simple and certainly popular dark matter candidate. The cross-section for such a WIMP, with velocity  $v$ , interacting with a Germanium target is [10]<sup>2</sup>

$$\frac{d\sigma}{dE_R} = \frac{m_{Ge} \sigma_n}{2v^2 \mu_n^2} A^2 F^2(q) \quad (1)$$

where  $\mu_n$  is the  $\chi$ -neutron reduced mass,  $\sigma_n$  is the  $\chi$ -neutron cross-section and  $F(q)$  is the form factor. Also,  $A$  is the mass number of the target nuclei, and isospin invariant  $\chi$  interactions have been assumed.

In addition to the cross-section, the interaction rate in a direct detection experiment also depends on the dark matter galactic halo distribution. Dark matter in the halo is generally assumed to be in a Maxwellian distribution:

$$f_\chi(\mathbf{v}_E, \mathbf{v}) = e^{-E/T} = e^{-(\mathbf{v}_E + \mathbf{v})^2/v_0^2} \quad (2)$$

where  $\mathbf{v}_E$  is the velocity of the Earth with respect to the halo, and  $\mathbf{v}$  is the velocity of the dark matter particles with respect to the Earth. In the standard halo model, the effective temperature of the Maxwellian distribution scales as the square of the galactic rotational velocity:  $T = \frac{1}{2} m_\chi v_{rot}^2$ . Evidently  $v_0 \equiv \sqrt{2T/m_\chi} = v_{rot}$ . We take the reference value  $v_{rot} = 230$  km/s since later we wish to compare with some results of ref.[19]. Also,  $|\mathbf{v}_E| = v_\odot + v_{orb} \cos \gamma \cos \omega(t - t_0)$ , with  $v_\odot = v_{rot} + 12$  km/s,  $v_{orb} = 30$  km/s,  $\cos \gamma = 0.5$  and  $t_0 = 152.5$  days (June 2<sup>nd</sup>). The velocity distribution is limited in this model by the galactic escape velocity, which we take as 600 km/s. That is,  $|\mathbf{v} + \mathbf{v}_E| < 600$  km/s.

The rate for  $\chi$  scattering on a Germanium target nucleus is

$$\frac{dR}{dE_R} = N_T n_\chi \int_{|\mathbf{v}| > v_{min}} \frac{d\sigma}{dE_R} \frac{f_\chi(\mathbf{v}, \mathbf{v}_E)}{k} |\mathbf{v}| d^3\mathbf{v} \quad (3)$$

where the integration limit is  $v_{min} = \sqrt{(m_{Ge} + m_\chi)^2 E_R / 2m_{Ge} m_\chi^2}$ . In Eq.(3),  $k = v_0^3 \pi^{3/2}$ ,  $N_T$  is the number of target nuclei and  $n_\chi = \rho_{dm} \xi_\chi / m_\chi$  is the number density of the halo  $\chi$  particles. [ $\rho_{dm} = 0.3$  GeV/cm<sup>3</sup> and  $\xi_\chi$  is the halo mass fraction of species  $\chi$ , generally assumed to be unity in single component dark matter models].

---

<sup>2</sup>Natural units,  $\hbar = c = 1$ , are used throughout.

*Hidden sector dark matter*

The other class of models we consider is where dark matter interacts with ordinary matter via a massless mediator. Dark matter from a hidden sector with  $U(1)'$  gauge interaction, coupling with ordinary matter via  $U(1)' - U(1)_Y$  kinetic mixing[15, 16] is a simple renormalizable example of such a model (which we henceforth adopt). If the  $U(1)'$  is unbroken then the kinetic mixing induces a tiny ordinary electric charge for the  $U(1)'$  charged particles[20]. This induced charge, denoted by  $\epsilon e$ , enables the hidden sector particles to elastically scatter off ordinary charged particles such as the nuclei in atoms. The cross-section for such a hidden sector particle of velocity  $v$  to thereby elastically scatter off a Germanium nucleus is given by[14]:

$$\frac{d\sigma}{dE_R} = \frac{2\pi\epsilon^2 Z_{Ge}^2 \alpha^2 F^2(q)}{m_{Ge} E_R^2 v^2} \tag{4}$$

where  $Z_{Ge} = 32$  is the atomic number of Germanium and  $\alpha$  is the fine structure constant. The most important difference between this Rutherford-type cross-section, and the one for standard WIMPs, Eq.(1), is the  $1/E_R^2$  dependence. It arises because the Feynman diagram for the elastic scattering process involving the exchange of a massless mediator<sup>3</sup> has amplitude proportional to  $1/q^2 \simeq 1/(2m_{Ge} E_R)$ .

Hidden sector dark matter has a number of other very distinctive properties. Firstly, such dark matter can have significant self-interactions mediated by the unbroken  $U(1)'$  gauge interaction. Secondly, it is also dissipative since a plasma composed of such particles can lose energy via radiating the  $U(1)'$  ‘dark’ photon in bremsstrahlung processes. A third distinctive feature of these kinds of models is that they are necessarily multi-component if the dark matter in the Universe arises from a particle-antiparticle asymmetry. This is due to the  $U(1)'$  neutrality of the Universe. See ref.[18] for further details and also ref.[22, 23] and references there-in for some relevant astrophysical/cosmological discussions of closely related models.

We consider the simplest such multi-component hidden sector model with two stable hidden sector particles,  $F_1$  and  $F_2$ <sup>4</sup>. The hydrostatic equilibrium condition on an isothermal spherical distribution of such particles implies[14, 25]:

$$v_0[F_i] = \sqrt{\frac{2T}{m_{F_i}}} = v_{rot} \sqrt{\frac{\bar{m}}{m_{F_i}}} \tag{5}$$

where  $\bar{m}$  is the mean mass of the particles in the halo. Thus for hidden sector dark matter, their halo distribution is still expected to be Maxwellian but  $v_0 \neq v_{rot}$ . If  $m_{F_2} \gg m_{F_1}$  it is possible to have  $m_{F_2} \gg \bar{m}$ , and hence  $v_0[F_2] \ll v_{rot}$ . This narrow

---

<sup>3</sup>If the mediator is not massless, but has mass  $m$ , then the Feynman amplitude is proportional to  $1/(q^2 + m^2)$ . Thus the cross-section is point-like or Rutherford-like depending on whether  $q^2 \ll m^2$  or  $q^2 \gg m^2$ . For the relevant recoil energies, the cross-section is approximately Rutherford-like,  $d\sigma/dE_R \propto 1/E_R^2$ , provided  $m \lesssim 10$  MeV. See ref.[21] for a study of the effect of varying  $m$ .

<sup>4</sup>It is supposed that the binding energy of any bound states that  $F_1$  and  $F_2$  might form is much less than the halo temperature  $T$ , a situation that is easy to satisfy. With this condition the halo is composed predominately of unbound  $F_1$  and  $F_2$  particles. The alternative case, where  $F_1$  and  $F_2$  form tightly bound ‘dark atoms’ has quite different phenomenology[24].

velocity dispersion of  $F_2$  can lead to a situation where lower threshold experiments, such as DAMA, CoGeNT are able to see  $F_2$  interactions while higher threshold experiments such as XENON100[26] and CDMS[27] do not. This can help explain why XENON100 and CDMS have yet to find a positive signal, even with  $F_2$  as heavy as  $\sim 50$  GeV[18].

The scattering rate of hidden sector  $F_2$  particles on target nuclei is of the same form as in Eq.(3), but with cross-section given in Eq.(4) and the  $v_0$  value given in Eq.(5). Note that for hidden sector dark matter, with significant self-interactions, the velocity distribution is not constrained by a galactic escape velocity limit.

### *Mirror dark matter*

Mirror dark matter corresponds to the interesting special case where the hidden sector is isomorphic to the standard model sector. The hidden sector, which we refer to as the mirror sector in this case, thus has gauge symmetry  $SU(3)' \otimes SU(2)'_L \otimes U(1)'_Y$ . The Lagrangian describing the ordinary and hidden sectors also respects an exact and unbroken  $Z_2$  mirror symmetry which can be interpreted as space-time parity[16]. The  $Z_2$  mirror symmetry interchanges each ordinary particle (scalar, fermions and gauge bosons) with a corresponding partner, denoted with a prime ( $'$ ). This discrete symmetry ensures that the fundamental properties of the hidden sector particles exactly mirror those of the ordinary sector. There is thus a spectrum of ‘mirror’ particles  $e'$ ,  $H'$ ,  $He'$ ,  $O'$ ,  $Fe'$ , .... The  $Z_2$  mirror symmetry ensures that the mass of each mirror particle is the same as the corresponding ordinary particle. For a more extensive treatment, including astrophysical and cosmological discussions, see the reviews[28] and references there-in.

Since the mirror sector is isomorphic to the standard model sector, the theory contains two gauged  $U(1)$  symmetries,  $U(1)_Y$  and  $U(1)'_Y$ . As discussed above for the generic hidden sector case, these two  $U(1)'_Y$ s can kinetically mix thereby inducing a small ordinary electric charge for the hidden sector charged particles. Thus, a mirror nucleus,  $A'$ , with atomic number  $Z'$  will couple to ordinary photons with electric charge  $\epsilon Z' e$ . Such a mirror nucleus moving with velocity  $v$  can thereby elastically scatter off an ordinary nucleus,  $A$ , with atomic number  $Z$ . This imparts an observable recoil energy,  $E_R$ , with

$$\frac{d\sigma}{dE_R} = \frac{2\pi\epsilon^2 Z^2 Z'^2 \alpha^2 F_A^2 F_{A'}^2}{m_A E_R^2 v^2} \quad (6)$$

where  $F_A$  [ $F_{A'}$ ] is the form factor of the nucleus [mirror nucleus].

In this theory, the galactic dark matter halo of the Milky Way is composed predominantly of mirror particles. These particles form a pressure supported, multi-component plasma containing  $e'$ ,  $H'$ ,  $He'$ ,  $O'$ ,  $Fe'$ ,...[25]. Each particle species is described by a Maxwellian distribution, but with velocity dispersion depending on the mass of the component, as in Eq.(5). In the mirror dark matter case,  $\bar{m}$  is not a free parameter, but constrained to be approximately 1.1 GeV from mirror BBN calculations[29].

### 3 Germanium spectrum - unmodulated part

Previous work[17, 18] has shown that the DAMA, CoGeNT and CRESST-II experiments can be simultaneously explained within the generic hidden sector framework as well as the more specific mirror dark matter case. These explanations are also consistent with the null results of other experiments such as XENON100[26] and CDMS[27], although not without some tension. These null results do suggest a narrow velocity dispersion of the detected dark matter particle  $F_2$ , i.e.  $\bar{m} \ll m_{F_2}$  in the two component hidden sector model considered here. The mean mass  $\bar{m}$  can be defined in terms of the abundances of  $F_1$  and  $F_2$ : via  $\bar{m} = (n_{F_1} m_{F_1} + n_{F_2} m_{F_2}) / (n_{F_1} + n_{F_2})$ . The  $U(1)'$  charge neutrality of a plasma of such particles implies  $q'_{F_1} n_{F_1} + q'_{F_2} n_{F_2} = 0$  where  $q'_{F_j}$  is the  $U(1)'$  charge of  $F_j$  ( $j = 1, 2$ ). Thus the condition  $\bar{m} \ll m_{F_2}$  implies that  $m_{F_1} \ll m_{F_2}$  and  $|q'_{F_1}| \ll |q'_{F_2}|$ . Such a situation is of course possible. [As briefly mentioned in the previous section, mirror dark matter for instance, predicts  $\bar{m} \approx 1.1$  GeV from mirror BBN calculations[29]]. The  $m_{F_1} \ll m_{F_2}$  requirement suggests that the experiments are only directly sensitive to interactions of the  $F_2$  component.

Fits to the DAMA annual modulation data implicate hidden sector dark matter mass in the range:  $m_{F_2} \gtrsim 20$  GeV (for  $v_{rot} = 230$  km/s) [18]. A rough upper limit,  $m_{F_2} \lesssim 60$  GeV is suggested by the null results of the XENON100 and CDMS direct detection experiments[18]. In figure 1 we examine the predicted Germanium recoil spectrum for  $F_2$  masses in this range, with the kinetic mixing parameter  $\epsilon$  adjusted so that the low energy normalization is fixed.

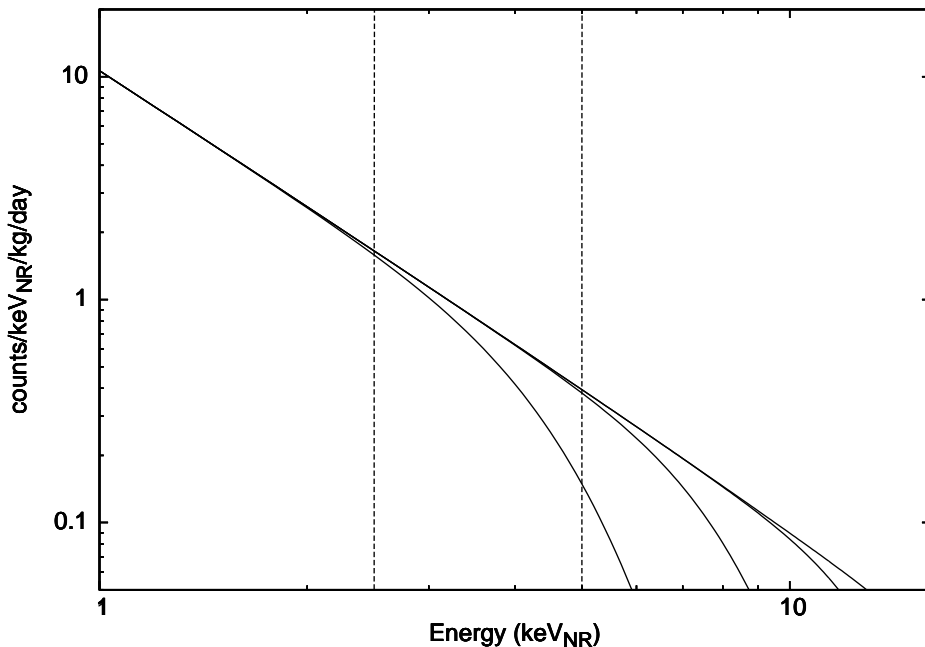


Figure 1: Germanium recoil spectrum from hidden sector dark matter. The lines from left to right correspond to  $m_{F_2}/\text{GeV} = 20, 30, 45, 60$ . [ $v_{rot} = 230$  km/s and  $\bar{m} = 1.0$  GeV]. The vertical dashed lines show the range of CoGeNT's low energy excess.

Figure 1 clearly demonstrates the expected  $dR/dE_R \propto 1/E_R^2$  behaviour at low energies of hidden sector dark matter. The energy threshold of the CoGeNT experiment is  $0.5 \text{ keVee} \approx 2.5 \text{ keV}_{NR}$ <sup>5</sup>. The CoGeNT low energy excess can be extracted from the background over the energy range:  $2.5 \text{ keV}_{NR} \lesssim E_R \lesssim 5 \text{ keV}_{NR}$ . For  $m_{F_2} \gtrsim 30 \text{ GeV}$ , the  $dR/dE_R \propto 1/E_R^2$  dependence extends throughout the entire CoGeNT low energy ‘signal’ region. For  $20 \text{ GeV} \lesssim m_{F_2} \lesssim 30 \text{ GeV}$  the shape of the spectrum can be somewhat steeper. A modest preference for  $m_{F_2} \gtrsim 30 \text{ GeV}$  arises[18] in this model from the relative normalizations of the DAMA and CoGeNT signals. With this justification, we now focus attention on hidden sector dark matter with  $m_{F_2} \gtrsim 30 \text{ GeV}$  for which the recoil energy spectral shape is ‘predicted’. [We comment later on the slight changes to the spectral shape if  $m_{F_2}$  is in the lower mass window  $20 \text{ GeV} \lesssim m_{F_2} \lesssim 30 \text{ GeV}$ ].

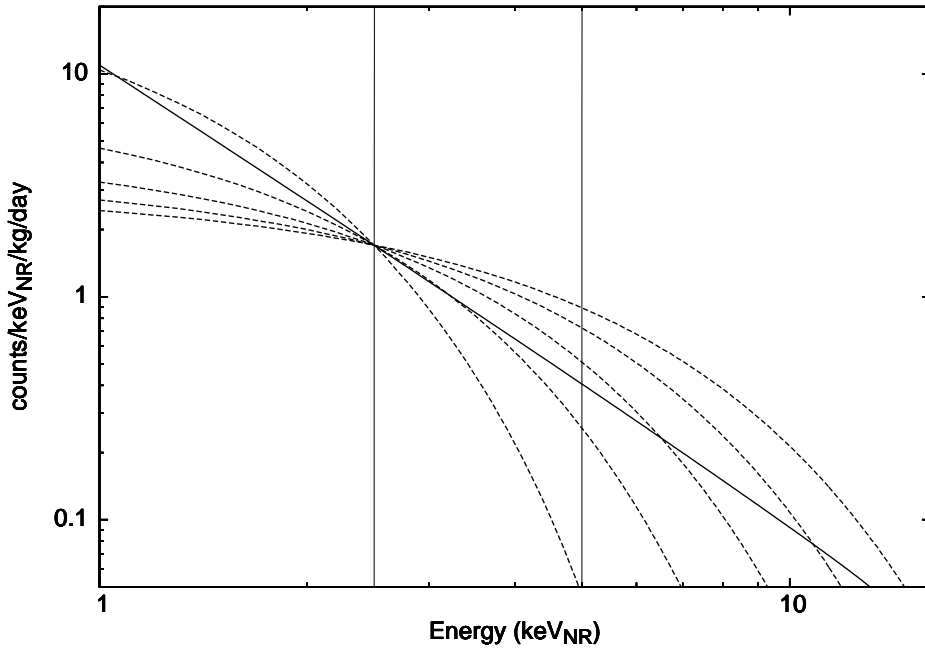


Figure 2: Comparison of the Germanium recoil spectrum predicted by hidden sector dark matter with that from light WIMPs. The solid line is the hidden sector prediction (for  $m_{F_2} \gtrsim 30 \text{ GeV}$ ) while dashed lines (from steepest to flattest) are predictions of light WIMPs for  $m_{\chi}/\text{GeV} = 6, 8, 10, 12, 14$ . The vertical dashed lines show the energy range of the CoGeNT excess and  $v_{rot} = 230 \text{ km/s}$  is assumed.

<sup>5</sup>The keVee unit refers to the measured ionization energy while  $\text{keV}_{NR}$  is the nuclear recoil energy equivalent. We assume that the quenching factor,  $q \equiv \text{keV}_{NR}/\text{keVee}$ , is given by  $q = 0.18(E_R/\text{keV}_{NR})^{0.12}$ . This is in between the value suggested by CoGeNT[4] and by the recent study[30]. It is also consistent with the experimental measurements summarized in figure 5 of ref.[4]. The uncertainty in the quenching factor, and thus CoGeNT’s nuclear recoil energy scale, is around 10-20%.

In figure 2, we compare the Germanium recoil spectrum of hidden sector dark matter with that obtained from light WIMPs. We adjust  $\sigma_n$  so that the rates have fixed normalization at 2.5 keV<sub>NR</sub>. Figure 2 shows that WIMPs with mass around  $m_\chi \approx 8$  GeV produce a Germanium recoil spectrum of similar shape to the  $dR/dE_R \propto 1/E_R^2$  dependence characteristic of hidden sector dark matter. To quantify this, we can define the ‘area’,  $\mathcal{A}(m_\chi)$  as:

$$\mathcal{A}(m_\chi) = \int_{2.5 \text{ keV}_{NR}}^{5 \text{ keV}_{NR}} \left| \frac{dR^{lw}}{dE_R} - \frac{dR^{hs}}{dE_R} \right| dE_R \quad (7)$$

where  $dR^{lw}/dE_R$  [ $dR^{hs}/dE_R$ ] is the rate in the light WIMP model [hidden sector model]. We find that  $\mathcal{A}(m_\chi)$  is minimized when  $m_\chi \simeq 8.5$  GeV. This means that for the energy range of CoGeNT’s excess, the scattering of  $m_\chi \simeq 8.5$  GeV WIMPs produces a recoil spectrum that most closely resembles the  $dR/dE_R \sim 1/E_R^2$  spectrum characteristic of hidden sector dark matter. This is illustrated in figure 3, along with CoGeNT’s data (corrected for efficiency, stripped of background components, and with surface event correction[4]).

Repeating this analysis for the low  $m_{F_2}$  mass window,  $20 \text{ GeV} \lesssim m_{F_2} \lesssim 30 \text{ GeV}$  we find that  $\mathcal{A}(m_\chi)$  is minimized for  $7.3 \text{ GeV} \lesssim m_\chi \lesssim 8.5 \text{ GeV}$ . Thus, there is only a very narrow  $m_\chi$  window where WIMPs can mimic the hidden sector dark matter spectral shape for the relevant CoGeNT energies.

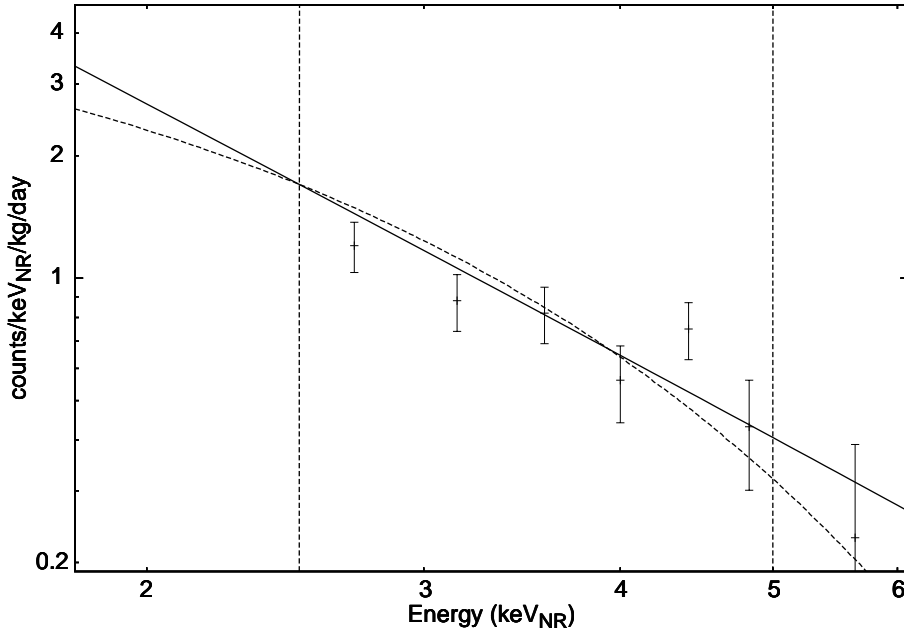


Figure 3: Comparison of the Germanium recoil spectrum predicted by hidden sector dark matter (solid line) with that from WIMPs with mass 8.5 GeV (dashed line). The vertical dashed lines show the energy range of the CoGeNT excess and  $v_{rot} = 230 \text{ km/s}$  is assumed. CoGeNT data, obtained from ref.[4], is also shown.



If hidden sector dark matter is correct then an analysis of the data in terms of light WIMPs should be consistent with  $7.3 \text{ GeV} \lesssim m_\chi \lesssim 8.5 \text{ GeV}$ . Systematic uncertainties due to calibration issues should be of order a GeV or less. In figure 4, we show an analysis of the CoGeNT and CDMS data in the light WIMP model. The CoGeNT analysis uses the most recent data from ref.[4] corresponding to  $0.33 \text{ kg} \times 807 \text{ days}$ . [This data is corrected for efficiency, stripped of known background components and with surface event correction]. Quenching factor uncertainties are taken into account as in ref.[18]. The CDMS data refers to the CDMS low energy data given in ref.[31]. This data covers roughly the same recoil energy range as CoGeNT's signal region [ $2.5 \text{ keV}_{NR} \lesssim E_R \lesssim 5 \text{ keV}_{NR}$ ]. Collar and Fields[19] carefully analysed this data and identified a family of events in the nuclear recoil band - a tentative dark matter signal. The analysis of ref.[19] reveals that the CDMS experiment pins down  $m_\chi$  fairly precisely due to its large exposure. The analysis of CDMS low energy data of ref.[19] could be repeated in the hidden sector framework. In lieu of that, it is useful to know the value of  $m_\chi$  for which the spectrum of light WIMPs approximately mimics that of hidden sector dark matter. Figure 4 shows that both the CoGeNT and CDMS data are consistent with  $m_\chi \simeq 8.5 \text{ GeV}$ . This can be viewed as interesting evidence in support of hidden sector dark matter.

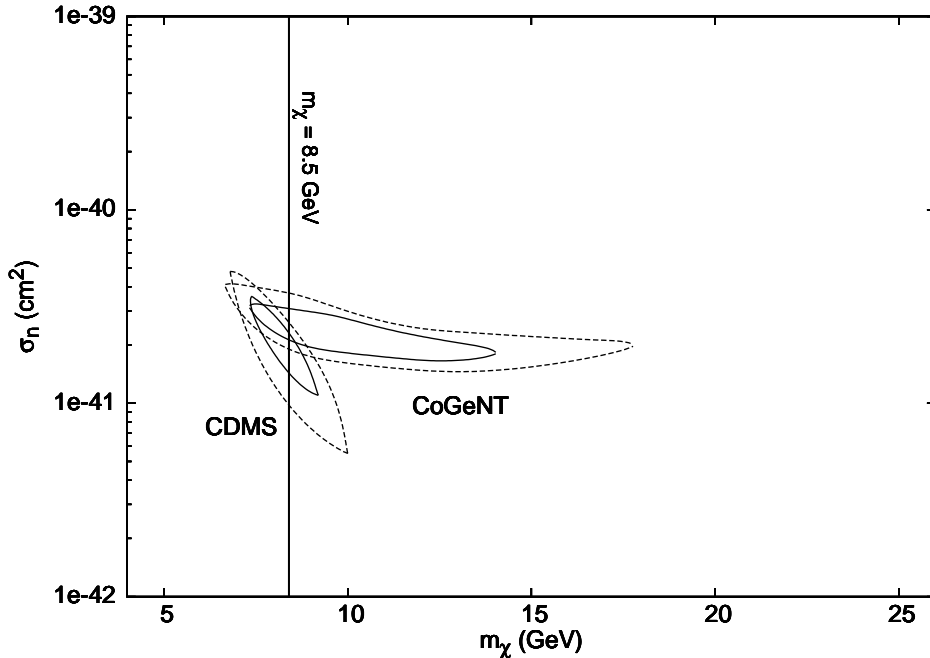


Figure 4: Favoured  $\sigma_n$ ,  $m_\chi$  parameter region [90% and 99% C.L.] in the light WIMP model for  $v_{rot} = 230 \text{ km/s}$ . The CDMS allowed regions are from ref.[19]. The vertical solid line indicates  $m_\chi = 8.5 \text{ GeV}$  - identified as the WIMP mass where the Ge recoil spectra most closely matches that of hidden sector dark matter ( $m_{F_2} \gtrsim 30 \text{ GeV}$ ).

$v_{rot}$	$m_\chi$	$\mathcal{A}_{min} \text{ kg}^{-1} \text{ day}^{-1}$
200 km/s	10.0 GeV	0.11
230 km/s	8.5 GeV	0.11
260 km/s	7.5 GeV	0.11

Table 1: The  $m_\chi$  value for which the scattering of WIMPs produces a Ge recoil spectrum that most closely resembles the  $dR/dE_R \sim 1/E_R^2$  spectrum of hidden sector dark matter (in the nuclear recoil energy region 2.5 keV<sub>NR</sub> - 5.0 keV<sub>NR</sub>).

The discussion so far has fixed  $v_{rot} = 230$  km/s. Varying  $v_{rot}$  away from this ‘reference’ value will not change the shape predicted in the hidden sector model. This is because the shape is governed by the  $d\sigma/dE_R \propto 1/E_R^2$  dynamics. However, for a fixed  $m_\chi$ , changing  $v_{rot}$  will change the predicted spectral shape in the light WIMP model. Thus, the value of  $m_\chi$  where light WIMPs most closely mimic hidden sector dark matter will change depending on the value of  $v_{rot}$  chosen (table 1). However, the value of  $m_\chi$  favoured by the data also changes and in roughly the same way. Thus our conclusions remain unchanged if we vary  $v_{rot}$ .

## 4 Germanium spectrum - modulated part

The dark matter interaction rate can be expanded in terms of an unmodulated and modulated part:

$$\frac{dR}{dE_R} = \frac{dR_0}{dE_R} + \frac{dR_1}{dE_R} \cos \omega(t - t_0) \quad (8)$$

where  $\omega = 2\pi/T$ ,  $T = 1$  year and  $t_0 = 152.5$  days. The previous section has dealt with the unmodulated part. Here we examine the expectations for the annual modulation amplitude,  $dR_1/dE_R$ . We study first the simplest hidden sector case, considered in the previous section, where only the  $F_2$  component is heavy enough to give significant contributions. In figure 5 we give the predicted annual modulation amplitude,  $dR_1/dE_R$ , for various values of  $m_{F_2}$ . Also shown is the annual modulation amplitude for WIMP dark matter with  $m_\chi = 8.5$  GeV. The cross-sections are normalized as in figures 1-3.

CoGeNT has reported some positive hints for an annual modulation in their event rate[3]. Meanwhile, CDMS[32] has constrained any modulation above 5 keV<sub>NR</sub>, to be less than around 0.05 counts/keV<sub>NR</sub>/kg/day. Figure 5 shows that all of the models considered predict a very small modulation amplitude above 5 keV<sub>NR</sub>, well within CDMS constraints. Figure 5 also indicates that the (minimal) hidden sector dark matter model considered predicts an annual modulation of negative sign at the lowest energies. This is not supported by CoGeNT’s initial measurements[3], which hint at a sizable positive amplitude  $dR_1/dE_R \sim 0.2$  counts/keV<sub>NR</sub>/kg/day averaged over the energy range 2.5 keV<sub>NR</sub> <  $E_R$  < 5 keV<sub>NR</sub>.

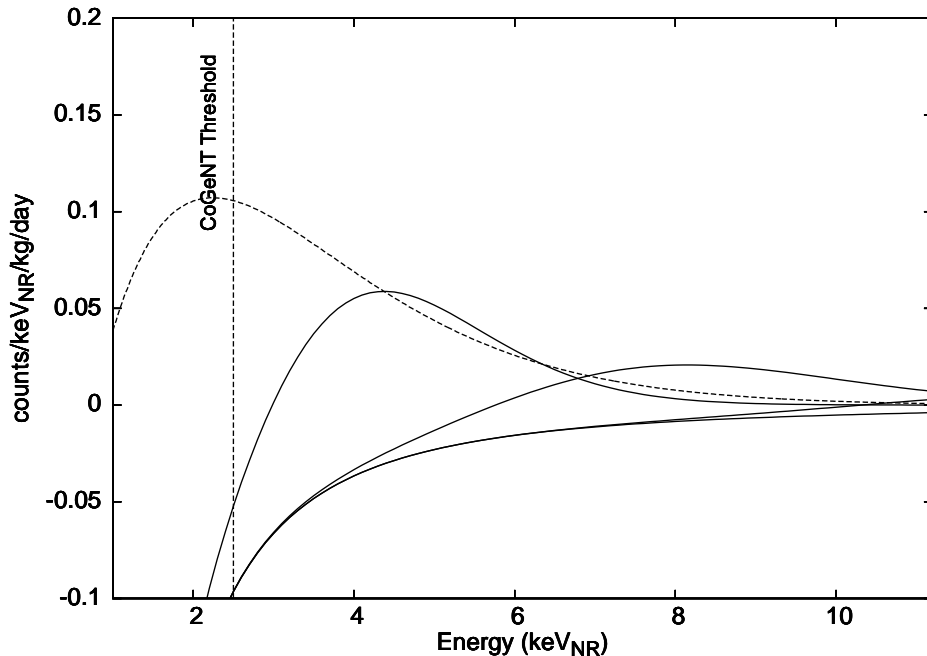


Figure 5: Annual modulation amplitude for  $m_\chi = 8.5$  GeV WIMP (dashed-line) and hidden sector dark matter with  $m_{F_2}/\text{GeV} = 20, 30, 45$  and  $60$  (solid lines from top to bottom). [ $v_{rot} = 230$  km/s and  $\bar{m} = 1.0$  GeV].

Hidden sector dark matter is expected to be multi-component and there might be light components giving positive contributions at low energies. Such a possibility is certainly expected in the specific mirror dark matter case. To illustrate this possibility we therefore consider the mirror dark matter model. Recall in that model a dark matter spectrum  $e', H', He', O', Fe', \dots$  with masses identical to their ordinary matter counterparts is predicted. The  $H'$  and  $He'$  components are too light to give an observable signal in any of the existing experiments. This leaves only the heavier mirror ‘metal’ components, which it happens, have roughly the right masses to explain the data.

It is, of course, very difficult to predict the heavy mirror element abundances in the Universe. However, since mirror ‘metal’ components are expected to be forged in mirror stars, a logical starting point might be to examine the ordinary metal abundances in the Universe. According to Wolfram[33], the eight most abundant metals in the Universe are: O, C, Ne, Fe, N, Si, Mg and S. Their abundances are given in table 2. If we assume that mirror metal abundances have a similar pattern then this motivates considering a mirror particle spectrum dominated by just four elements: <sup>6</sup>

---

<sup>6</sup>We arrive at these four elements by observing that (a) the carbon contribution is suppressed via kinematic effects relative to oxygen and can be approximately discarded, (b) N,O have similar mass which we approximate with O and (c) Mg, Si, S have mass number  $28 \pm 4$ , so that these can be roughly approximated by just Si.

element	metal mass fraction
Oxygen [O]	0.48
Carbon [C]	0.24
Neon [Ne]	0.07
Iron [Fe]	0.06
Nitrogen [N]	0.05
Silicon [Si]	0.04
Magnesium [Mg]	0.03
Sulfur [S]	0.02

Table 2: The eight most abundant metals in the Universe. The metal mass fraction of nuclei  $A_1$  is  $\xi_{A_1}/\sum \xi_A$  where the sum runs over all elements except H and He.

$O'$ ,  $Ne'$ ,  $Si'$ ,  $Fe'$ , with metal mass fractions given by

$$(a) \quad \frac{\xi_{O'}}{\mathcal{N}} = 0.7, \quad \frac{\xi_{Ne'}}{\mathcal{N}} = 0.1, \quad \frac{\xi_{Si'}}{\mathcal{N}} = 0.1, \quad \frac{\xi_{Fe'}}{\mathcal{N}} = 0.1 \quad (9)$$

where  $\mathcal{N} \equiv \sum \xi_{A'}$  and the sum runs over all mirror elements except  $H'$ ,  $He'$ . We also consider two alternative examples. The first gives more weight to heavier components, while the second more to lighter components:

$$(b) \quad \frac{\xi_{O'}}{\mathcal{N}} = 0.5, \quad \frac{\xi_{Ne'}}{\mathcal{N}} = 0.05, \quad \frac{\xi_{Si'}}{\mathcal{N}} = 0.2, \quad \frac{\xi_{Fe'}}{\mathcal{N}} = 0.25 ,$$

$$(c) \quad \frac{\xi_{O'}}{\mathcal{N}} = 0.8, \quad \frac{\xi_{Ne'}}{\mathcal{N}} = 0.12, \quad \frac{\xi_{Si'}}{\mathcal{N}} = 0.08, \quad \frac{\xi_{Fe'}}{\mathcal{N}} = 0 . \quad (10)$$

It is expected that more stellar processing in larger mirror stars should increase the proportion of heavier metal components. The three sets (a), (b) and (c) (above) aim to illustrate the range of possible values for the abundances. More extreme ranges are, of course, possible.

In figure 6a,b we plot the Germanium recoil spectrum and annual modulation amplitude for mirror dark matter with the three different sets of abundances (a), (b) and (c). We assume  $\bar{m} = 1$  GeV and  $v_{rot} = 230$  km/s for the (a) abundance set,  $v_{rot} = 200$  km/s for the (b) abundance set and  $v_{rot} = 270$  km/s for the (c) abundance set. We also show the corresponding spectra for  $m_\chi = 8.5$  GeV WIMPs ( $v_{rot} = 230$  km/s).

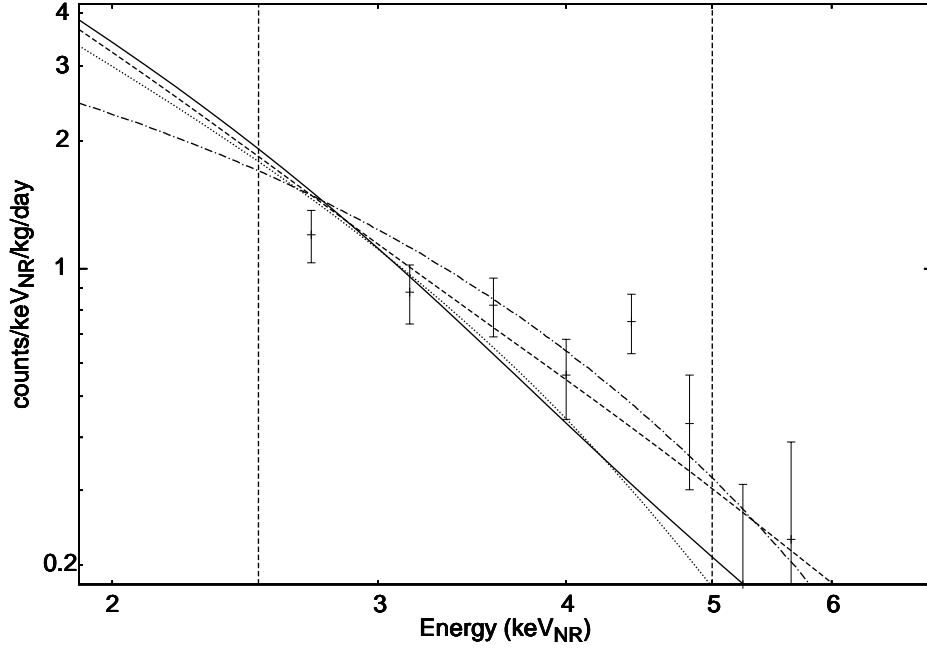


Figure 6a: Germanium spectrum with mirror dark matter for: the (a) abundances [solid line], (b) abundances [dashed line] and (c) abundances [dotted line] (see text). Also shown is the spectra for  $m_\chi = 8.5$  GeV WIMP model [dashed-dotted line]. The parameters  $\epsilon$  and  $\sigma_n$  are adjusted so that the curves have similar normalization in the CoGeNT signal region.

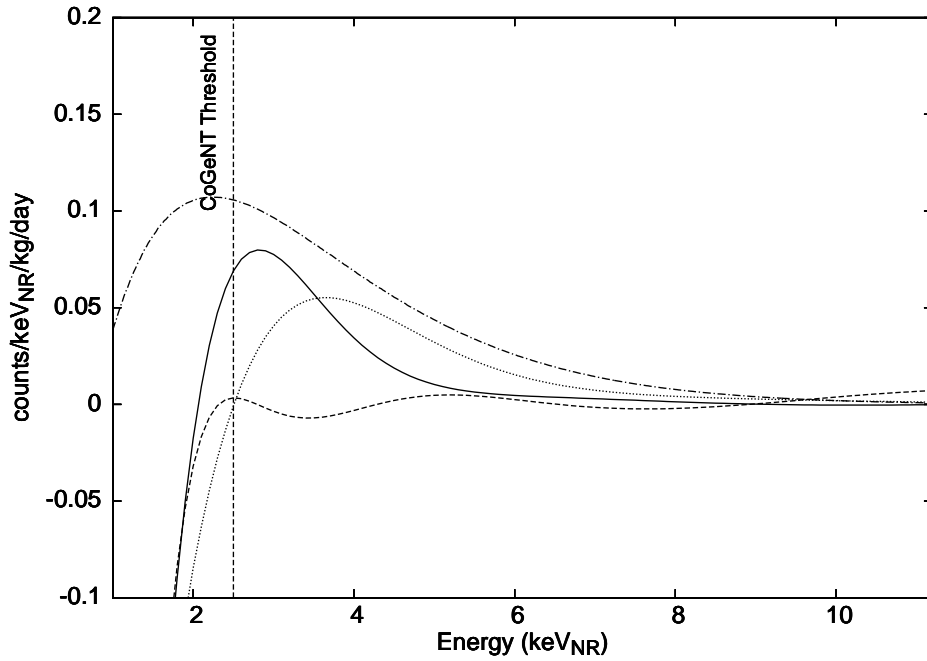


Figure 6b: Annual modulation amplitude for the same cases and parameters as figure 6a.

Figures 6a,b indicate that each of these examples can fit the data, with the (b) abundances slightly preferred by CoGeNT's spectrum. In each case the annual modulation amplitude is quite small in CoGeNT, with the (a), (c) abundances able to give a small positive contribution at low energies [essentially this is due to the larger  $O'$  proportion]. Each of these examples has just one free parameter, which can be taken as the product:  $\epsilon\sqrt{\xi_{O'}}$ . The normalization of the CoGeNT spectrum fixes this free parameter:  $\epsilon\sqrt{\xi_{O'}} \approx 4 \times 10^{-10}$  for the (a), (c) abundance set and  $\epsilon\sqrt{\xi_{O'}} \approx 2.4 \times 10^{-10}$  for the (b) abundance set. With this parameter fixed, I have checked that the examples with (a) and (b) abundances also give a reasonable fit to the DAMA annual modulation spectrum and the CRESST-II excess (when analysed as in ref.[17]). The example with (c) abundance can fit the DAMA annual modulation signal but gives too few events for CRESST-II. These examples illustrate the substantial parameter space whereby mirror dark matter can simultaneously explain the three positive dark matter signals.

Although the size of the annual modulation signal predicted in figures 5 and 6b is fairly small, there are nevertheless excellent prospects that it can be measured (or strongly constrained). The C-4[7], CDEX[8], and the MAJORANA demonstrator[9] experiments plan Germanium target mass  $\sim 4$  kg, 10 kg and 40 kg respectively. This is orders of magnitude larger than CoGeNT's  $\sim 0.3$  kg target. This should be sufficient to distinguish hidden sector dark matter from light WIMPs via the annual modulation signal. This should complement the information obtained from precise measurements of the unmodulated recoil spectrum considered in the previous section.

## 5 Conclusion

Current data from the DAMA, CoGeNT and CRESST-II experiments can potentially be explained within several dark matter frameworks. The most promising of which appears to be light WIMP dark matter and hidden sector dark matter. Both of these approaches feature spin independent elastic scattering of dark matter particles on nuclei. However light WIMP dark matter invokes a single particle species that interacts with ordinary matter via contact interactions, while hidden sector dark matter is typically multi-component and is assumed to interact via the exchange of a massless mediator.

We have examined and compared the predictions of hidden sector dark matter with that of light WIMPs for experiments using Germanium detectors, such as CoGeNT, and in the near future, C-4, CDEX and the MAJORANA demonstrator. Hidden sector dark matter predicts a spectrum:  $dR/dE_R \propto 1/E_R^2$  or even more steeply falling if the threshold of light components is passed. Scattering of light WIMPs, on the other hand, produce a recoil spectrum which depends sensitively on the WIMP mass  $m_\chi$ , with  $dR/dE_R \rightarrow \text{constant}$  as  $E_R \rightarrow 0$ . For the energy range of CoGeNT's excess, WIMPs with  $m_\chi \simeq 8.5$  GeV produce a recoil spectrum that approximately matches the  $\sim 1/E_R^2$  dependence characteristic of hidden sector models. The WIMP model fit to the CoGeNT excess, and also an analysis[19] of low energy CDMS data, favour  $m_\chi \approx 8.5$  GeV. This 'coincidence' can be viewed as interesting evidence in support of

hidden sector dark matter.

Future experiments should be able to differentiate hidden sector dark matter from light WIMPs, even for a WIMP mass of 8.5 GeV. The C-4 experiment[7] for instance, which aims to have a lower threshold and reduced background should be able to probe the signal over a significantly wider energy range. The characteristic flattening of the predicted WIMP spectrum at low energies, absent for hidden sector dark matter, is one way. Another way is via the annual modulation signal. We have shown that the two scenarios generally give different annual modulation spectra. This should provide another means to distinguish light WIMPs from hidden sector dark matter.

## Acknowledgments

The author thanks M. Schmidt for a useful comment. This work was supported by the Australian Research Council.

## References

- [1] R. Bernabei *et al.*, Riv. Nuovo Cim. **26N1**, 1 (2003) [astro-ph/0307403]; Int. J. Mod. Phys. D **13**, 2127 (2004) [astro-ph/0501412]; Phys. Lett. B **480**, 23 (2000).
- [2] R. Bernabei *et al.* [DAMA and LIBRA Collaborations], Eur. Phys. J. C **67**, 39 (2010) [arXiv:1002.1028]; Eur. Phys. J. C **56**, 333 (2008) [arXiv:0804.2741].
- [3] C. E. Aalseth *et al.* [CoGeNT Collaboration], Phys. Rev. Lett. **107**, 141301 (2011) [arXiv:1106.0650]; Phys. Rev. Lett. **106**, 131301 (2011) [arXiv:1002.4703].
- [4] C. E. Aalseth *et al.* [CoGeNT Collaboration], arXiv:1208.5737.
- [5] G. Angloher *et al.*, Eur. Phys. J. C **72**, 1971 (2012) [arXiv:1109.0702].
- [6] A. K. Drukier, K. Freese and D. N. Spergel, Phys. Rev. D **33**, 3495 (1986).  
K. Freese, J. A. Frieman and A. Gould, Phys. Rev. D **37**, 3388 (1988).
- [7] R. M. Bonicalzi *et al.* [C-4 Collaboration], arXiv:1210.6282.
- [8] Q. Yue *et al.* [CDEX-TEXONO Collaboration], arXiv:1201.5373.
- [9] G. K. Giovanetti *et al.*, J. Phys. Conf. Ser. **375**, 012014 (2012).
- [10] J. D. Lewin and P. F. Smith, Astropart. Phys. **6**, 87 (1996).
- [11] D. Hooper, J. I. Collar, J. Hall, D. McKinsey and C. Kelso, Phys. Rev. D **82**, 123509 (2010) [arXiv:1007.1005].
- [12] C. Savage, G. Gelmini, P. Gondolo and K. Freese, JCAP **0904**, 010 (2009) [arXiv:0808.3607]; P. Gondolo and G. Gelmini, Phys. Rev. D **71**, 123520 (2005) [hep-ph/0504010].

- [13] C. Savage, G. Gelmini, P. Gondolo and K. Freese, Phys. Rev. D **83**, 055002 (2011) [arXiv:1006.0972]; Y. Mambrini, JCAP **1009**, 022 (2010) [arXiv:1006.3318]; P. J. Fox, J. Liu and N. Weiner, Phys. Rev. D **83** (2011) 103514 [arXiv:1011.1915]; J. L. Feng, J. Kumar, D. Marfatia and D. Sanford, Phys. Lett. B **703**, 124 (2011) [arXiv:1102.4331]; C. Arina, J. Hamann and Y. Y. Y. Wong, JCAP **1109**, 022 (2011) [arXiv:1105.5121]; D. Hooper and C. Kelso, Phys. Rev. D **84**, 083001 (2011) [arXiv:1106.1066]; P. Belli, R. Bernabei, A. Bottino, F. Cappella, R. Cerulli, N. Fornengo and S. Scopel, Phys. Rev. D **84**, 055014 (2011) [arXiv:1106.4667]; T. Schwetz and J. Zupan, JCAP **1108**, 008 (2011) [arXiv:1106.624]; M. Farina, D. Pappadopulo, A. Strumia and T. Volansky, JCAP **1111**, 010 (2011) [arXiv:1107.0715]; J. Kopp, T. Schwetz and J. Zupan, JCAP **1203**, 001 (2012) [arXiv:1110.2721]; C. Kelso, D. Hooper and M. R. Buckley, Phys. Rev. D **85**, 043515 (2012) [arXiv:1110.5338]; M. T. Frandsen, F. Kahlhoefer, C. McCabe, S. Sarkar and K. Schmidt-Hoberg, JCAP **1201**, 024 (2012) [arXiv:1111.0292]; J. M. Cline, Z. Liu and W. Xue, arXiv:1207.3039 [hep-ph].
- [14] R. Foot, Phys. Rev. D **69**, 036001 (2004) [hep-ph/0308254]; Mod. Phys. Lett. A **19**, 1841 (2004) [astro-ph/0405362]; astro-ph/0403043; Phys. Rev. D **82**, 095001 (2010) [arXiv:1008.0685]; Phys. Lett. B **692**, 65 (2010) [arXiv:1004.1424]; Phys. Lett. B **703**, 7 (2011) [arXiv:1106.2688].
- [15] R. Foot and X-G. He, Phys. Lett. B **267**, 509 (1991).
- [16] R. Foot, H. Lew and R. R. Volkas, Phys. Lett. B **272**, 67 (1991); Mod. Phys. Lett. A **7**, 2567 (1992); R. Foot and R. R. Volkas, Phys. Rev. D **52**, 6595 (1995) [hep-ph/9505359].
- [17] R. Foot, Phys. Rev. D **86**, 023524 (2012).
- [18] R. Foot, arXiv:1209.5602.
- [19] J. I. Collar and N. E. Fields, arXiv:1204.3559.
- [20] B. Holdom, Phys. Lett. B **166**, 196 (1986).
- [21] N. Fornengo, P. Panci and M. Regis, Phys. Rev. D **84**, 115002 (2011) [arXiv:1108.4661].
- [22] J. L. Feng, M. Kaplinghat, H. Tu and H. -B. Yu, JCAP **0907**, 004 (2009) [arXiv:0905.3039].
- [23] N. F. Bell, K. Petraki, I. M. Shoemaker and R. R. Volkas, Phys. Rev. D **84**, 123505 (2011) [arXiv:1105.3730]; K. Petraki, M. Trodden and R. R. Volkas, JCAP **1202**, 044 (2012) [arXiv:1111.4786].
- [24] J. M. Cline, Z. Liu and W. Xue, Phys. Rev. D **85**, 101302 (2012) [arXiv:1201.4858].
- [25] R. Foot and R. R. Volkas, Phys. Rev. D **70**, 123508 (2004) [astro-ph/0407522].



- [26] E. Aprile *et al.* [XENON100 Collaboration], arXiv:1207.5988.
- [27] Z. Ahmed *et al.* [CDMS-II Collaboration], Science **327**, 1619 (2010) [arXiv:0912.3592].
- [28] A. Y. Ignatiev and R. R. Volkas, hep-ph/0306120; R. Foot, Int. J. Mod. Phys. D **13**, 2161 (2004) [astro-ph/0407623]; Int. J. Mod. Phys. A **19**, 3807 (2004) [astro-ph/0309330]; Z. Berezhiani, Int. J. Mod. Phys. A **19**, 3775 (2004) [hep-ph/0312335]; P. Ciarcelluti, Int. J. Mod. Phys. D **19**, 2151 (2010) [arXiv:1102.5530].
- [29] P. Ciarcelluti and R. Foot, Phys. Lett. B **690**, 462 (2010) [arXiv:1003.0880].
- [30] D. Barker and D. -M. Mei, arXiv:1203.4620.
- [31] Z. Ahmed *et al.* [CDMS-II Collaboration], Phys. Rev. Lett. **106**, 131302 (2011) [arXiv:1011.2482].
- [32] Z. Ahmed *et al.* [CDMS Collaboration], arXiv:1203.1309.
- [33] <http://www.wolframalpha.com/>